Ion Tracks in Metals and Intermetallic Compounds

A. Barbu, H. Dammak, A. Dunlop, and D. Lesueur

Introduction

When an energetic ion penetrates a target, it loses its energy via two nearly independent processes: (1) elastic collisions with the nuclei (nuclear-energy loss $(dE/dx)_n$), which dominate the ion slowing down in the low energy range (i.e., in the stopping region); (2) electronic excitation and ionization (electronic-energy loss $(dE/dx)_e$), which strongly overwhelm $(dE/dx)_n$ in the high energy range (typically above 1 MeV/nucleon). Until the 1980s, researchers considered that electronic-energy deposition could participate in damaging creation in many insulators,[1] but the effects observed in bulk metals were solely ascribed to elastic nuclear collisions. This widely held opinion was due to the fact that in metallic systems the numerous very mobile conduction electrons allow a fast spreading of the deposited energy and an efficient screening of the space charge created in the projectile wake so that it seemed unreasonable to hope for damage creation or track formation in metallic targets following high levels of electronic-energy deposition.

A particular case is the observation more than 30 years ago of damage in thin[2] or discontinuous[3,4] metallic films after fission fragment irradiation or MeV heavy ion bombardment. The spreading of the deposited energy is then strongly limited by the close vicinity of surfaces and interfaces.

The recent development of swift, heavy ion accelerators (such as GSI-Darmstadt and GANIL-Caen, delivering a few 10 MeV/nucleon O to U beams) has allowed (1) use of well-defined parallel beams; (2) work in a regime in which the following conditions are realized: $(dE/dx)_e \approx 1$ to 80 keV/nm, $(dE/dx)_e/(dE/dx)_n \approx 2{,}000$, which are very favorable to study damage creation induced by high $(dE/dx)_e$; and (3) study of $(dE/dx)_e$ effects in bulk targets due to the very large range (a few tens to 100 μm) of such projectiles. It was thus very tempting to determine whether in such extreme conditions, it was possible to induce some damage in metallic targets following high electronic-energy deposition. In fact, quite a few unexpected microstructural modifications, to be described in more detail later, could be evidenced. They are seen in materials that exist in various stable or metastable phases.

The easiest observation is the transformation from a crystalline state to an amorphous one. (Amorphous latent tracks are seen in some intermetallic compounds, similar to what was observed long ago in some insulators.)[1]

Microstructural changes can also occur in materials that have various allotropic forms. Defective crystalline "tracks" are observed in a few pure metals and lead, for example, in titanium to a phase transformation from a crystalline phase to another crystalline phase at high irradiation fluences.

All these effects that are due to high electronic excitations will result in microstructural modifications localized in the close vicinity of the projectile paths and will hereafter be named "tracks." In most cases, they will be evidenced directly by transmission electron microscopy or indirectly considering their consequences, using, for example, small angle x-ray scattering or differential chemical attack of the damaged zones (as currently used in insulators).

Amorphous Tracks in Metallic Crystalline Compounds

The first tracks in bulk metallic materials were observed a few years ago in intermetallic alloys. Two classes of compounds have been studied:

(1) The first class consists of compounds that are known to be easily amorphized by elastic collisions during irradiations with low-energy ions or MeV electrons.[5] Among them, $NiZr_2$, NiTi, and Ni_3B are of particular interest. All of them are characterized by low local symmetry. Ni_3B and $NiZr_2$ have, respectively, orthorhombic and tetragonal crystallographic structures over the complete temperature range whereas NiTi experiences a martensitic transformation at a temperature that depends on the thermomechanical treatments but lies close to 300 K. NiTi is in a cubic B2 phase above the transition temperature and in a monoclinic phase below.

(2) The second class consists of compounds that are characterized by high local symmetry (LI_2 crystallographic structure). They include Zr_3Al, which is rather difficult to amorphize by elastic collisions,[6] and Cu_3Au, which has never been amorphized by any method, but which can be chemically disordered during low-temperature irradiations in the elastic collision regime.

In the second class of compounds, the only observable damage could be accounted for by elastic collisions[7-9] whereas sufficiently high levels of electronic-energy deposition induce amorphous track formation in the first class of compounds.

The Simple Cases of $NiZr_2$ and Ni_3B

In $NiZr_2$,[8,10,11] latent tracks are observed at 300 K in the electron microscope after GeV ion irradiations at 80 or 300 K at fluences of a few 10^{11} ions/cm^2 as soon as $(dE/dx)_e$ is high enough. Using xenon ions ($(dE/dx)_e \approx 30$ keV/nm), no contrast of latent track is observed in the irradiated sample whereas using lead ions ($(dE/dx)_e \approx 48$ keV/nm), discontinuous to quasicontinuous latent tracks are visible (Figure 1). Finally, after uranium irradiation ($(dE/dx)_e \approx 54$ keV/nm), almost continuous tracks are imaged. In Figure 1a, the density of dots (tracks seen from above) is equal to the impinging ion fluence. From Figure 1b, which is a view of the same area tilted 20°, the result is that the damage extends through the whole sample thickness and that the contrast and the diameter vary along the ion path. Finally, electron diffraction shows that partial amorphization of the material occurred and that amorphous matter indeed lies inside the damaged cylinders.

Very similar results were obtained in Ni_3B targets[12,13] in which amorphous latent tracks are observed following high

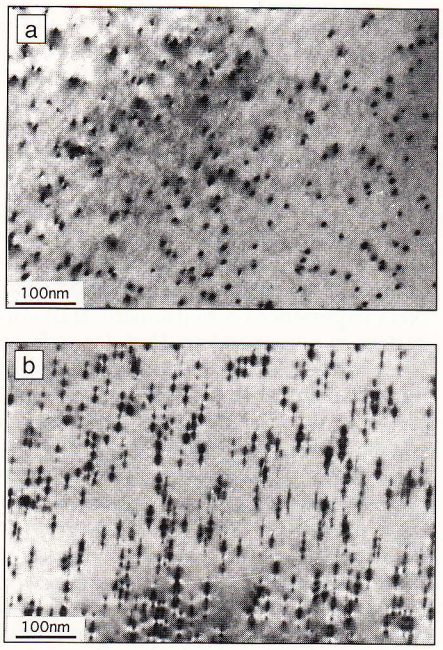

Figure 1. Bright-field electron micrograph of a $NiZr_2$ sample irradiated at 300 K with 0.7 GeV lead ions up to a fluence of 10^{11} cm^{-2}. (a) The electron-beam direction is parallel to the ion beam. (b) The sample is tilted 20° in the electron microscope.

$(dE/dx)_e$ levels, with the limitation that these tracks are not stable at room temperature. A few months after irradiation, no more tracks are visible in the irradiated samples whereas this phenomenon does not occur in irradiated $NiZr_2$ targets. It thus seems to be easy to reconstruct, at room temperature, crystalline matter inside the amorphized cylindrical zones of Ni_3B targets.

A More Puzzling Situation: The Shape Memory Compound NiTi

Considering the possibility of changing both (1) the martensitic transition temperature in NiTi from the low-temperature monoclinic structure to the high-temperature cubic structure according to thermomechanical treatments and (2) the irradiation temperature, irradiations could be performed in either one of the structures or in samples in which both phases coexisted.[11,14,15] The main result is that the sensitivities of the cubic and monoclinic phases to electronic excitations are surprisingly different. Above a $(dE/dx)_e$ threshold ≈ 48 keV/nm, tracks are observed, but only in the regions of the sample that were in the monoclinic phase during the irradiation. Figure 2a is an electron micrograph of a sample in which both phases were present in the irradiation conditions. Tracks are observed in the monoclinic lathe but not in the surrounding cubic matrix. Figure 3 presents amorphous tracks observed in the cubic phase of a NiTi sample that was irradiated with GeV uranium ions in the monoclinic phase. The tracks, created in the low-temperature phase, are very well-defined, have a diameter of 12 nm, and consist of homogeneously damaged cylinders. They are amorphous, as shown by electron diffraction, and stay stable when the sample transforms back into the cubic structure as the temperature is brought back to 300 K. The existence of numerous amorphous tracks does not seem to hamper the phase change. This structural stability of the tracks is strong. As some shearing occurs during the phase change, an apparent tipping over of the tracks is induced. Figure 2b is relative to a sample that was irradiated in the monoclinic phase at 80 K; tracks were induced in the whole sample. When the sample was subsequently heated to room temperature, the transition to the cubic phase occurred. During this transition, a rotation of a few degrees between the various monoclinic lathes took place. At the observation temperature, the matrix was totally in the cubic phase. The amorphous tracks are found slightly misaligned as a memory of the apparent tipping-over just described. If the sample is brought back again in the monoclinic phase by lowering the temperature, the tracks realign. The tracks act here as markers of the displacive phase transformation.

These results can be summarized as follows: Amorphous latent tracks observable at 300 K in an electron microscope can be formed in metallic compounds as soon as the energy deposited in electronic excitation is sufficient. As in insulators, when $(dE/dx)_e$ increases above the threshold, the configuration of the tracks gradually evolves from strings of separated, damaged droplets to more or less continuously damaged cylinders. The $(dE/dx)_e$ threshold strongly depends on the nature of the target (≈40–50 keV/nm in $NiZr_2$, Ni_3B, and NiTi, certainly much higher if it exists in Zr_3Al), but in all cases the high values of these thresholds (compared to typically a few keV/nm in insulators) explain why latent tracks in metallic targets were seen only recently. Finally, it seems that tracks are formed more easily in compounds showing a very low local symmetry.

"Tracks" in Pure Metals

The study of the influence of high electronic-energy deposition on damage processes in pure metals is not as easy as in metallic compounds, as there is certainly no chance to induce any amorphous tracks in metals by such methods. Most of the experiments consisted of low-temperature GeV heavy ion irradiations of thin metallic ribbons. The target thickness (a few μm) was always such that the stopping region of the projectiles was carefully avoided. This allows study in a regime in which the projectiles are mostly slowed down in electronic processes. The *in situ* measurement of the electrical resistivity of the samples during the irradiation allows the determination of the cross section σ_d for damage creation during the bombardment. Nuclear collisions are always present. The

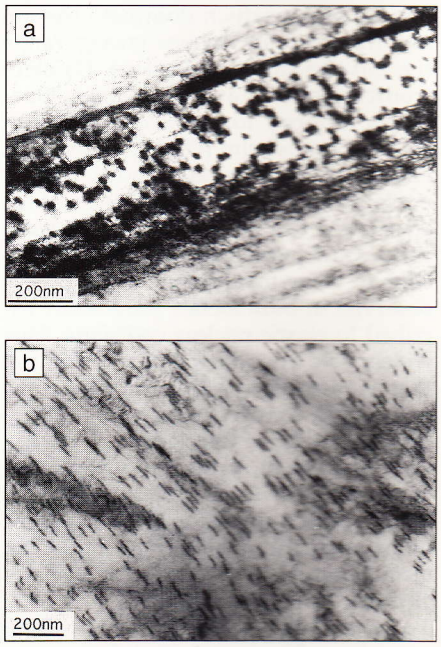

Figure 2. (a) Bright-field electron micrograph of a NiTi sample irradiated at 300 K with 0.84 GeV lead ions ($(dE/dx)_e \approx 52$ keV/nm) up to a fluence of 10^{11} cm^{-2}. Latent tracks are only visible in the monoclinic lathe and not in the surrounding matrix, which was in the cubic phase during irradiation. (b) Bright-field electron-microscopy observation at 300 K of a NiTi sample irradiated at 80 K in the monoclinic phase with 0.76 GeV uranium ions ($(dE/dx)_e \approx 57$ keV/nm) up to a fluence of 5×10^{10} cm^{-2}. The rotation of the tracks described in the text is visible.

cross section σ_n for damage creation in these elastic processes can be calculated.[16] Figure 4 presents the evolution of the ratio $\xi = \sigma_d/\sigma_n$ (referred to as the damage efficiency) of the measured to the calculated cross sections as a function of the linear rate of electronic-energy deposition $(dE/dx)_e$. If electronic processes were inoperant in the targets, then the measured and calculated cross sections should be equal. This is what is observed in a few targets, such as Cu, W, and Ag, in which damage results solely from elastic collisions.[17,18]

Iron

Iron has a particular behavior detailed in Figure 4.[19] Two different regimes are clearly visible. In region I, below 40 keV/nm, the efficiency decreases monotonically. In region II, above 40 keV/nm, a spectacular increase of ξ is observed. The proposed explanation is as follows:

(1) In region I, the amount of damage introduced in the sample is smaller than that resulting from elastic collisions only, which indicates that part of the energy deposited in electronic excitation is converted into atomic motion leading to a partial recombination of the defects just created.

(2) In region II, the measured damage increases strongly and overwhelms that expected from elastic processes. This indicates that a new mechanism of damage production appears. This additional damage is a direct consequence of electronic deposition that is able, when sufficiently high, to displace lattice atoms from their sites. Isochronal annealing of this damage indicates that we mainly deal with the creation of isolated point defects and thus, that no tracks are formed. This is confirmed by the fact that no contrast due to defect clusters could be seen in the electron microscope.

Titanium

Considering Figure 4 again, three metals seem to be particularly easy to damage when submitted to electronic-energy deposition: Ti, Co, and Zr. These three metals have a strong similarity: They all exist in various allotropic forms, which should favor eventual phase changes under high $(dE/dx)_e$. We shall now detail the results obtained in titanium, which is the most sensitive of all. Electron-microscopy observations were performed after low-temperature irradiations in the fluence range of 10^{11}–10^{13} cm^{-2} with O to U GeV ions.[20–22]

At low $(dE/dx)_e$ (<26 keV/nm), no damage is visible in the electron microscope. At higher $(dE/dx)_e$, after irradiation at moderate fluences ($\approx 10^{11}$ cm^{-2}), "tracks" are observable. Figure 5 presents micrographs of a Ti sample irradiated at 20 K with 2.2 GeV U ions ($(dE/dx)_e \approx 39$ keV/nm) up to a fluence of 2.5×10^{11} cm^{-2}. The density of visible objects in Figure 5a corresponds to the impinging ion fluence. Figure 5b shows damaged zones aligned along the ion-beam direction independent of the crystallographic orientation in the target. (A grain boundary is visible in the center of Figure 5b). The damage is once again strongly localized along the ion wake, that is, in the region in which electronic-energy deposition is the most important. The damaged zones are not amorphous. They could consist of dislocation loops lying in the prismatic planes of the hcp structure of Ti.[20,22]

In the same irradiation conditions, but at higher fluences, that is, when the damaged zones spatially overlap, a phase change to another crystalline phase occurs. The sample evolves from the usual hcp α-phase to the hexagonal ω-phase, as shown by x-ray diffraction (Figure 6) and electron microscopy. (New spots characteristic of this new phase appear on the electron-diffraction pattern; ω-domains are imaged.)[21] This ω-phase is the high-pressure phase of Ti, which is usually obtained from the α-phase when either a static or a dynamic pressure is applied. Due to the wide hysteresis of the

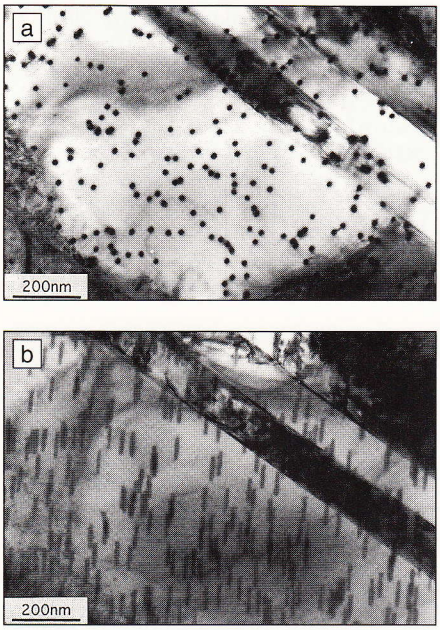

Figure 3. Bright-field electron micrograph of a NiTi sample irradiated in the monoclinic phase at 90 K with 0.76 GeV uranium ions ($(dE/dx)_e \approx 57$ keV/nm) up to a fluence of 5×10^{10} cm^{-2}. Very well-defined amorphous latent tracks are imaged at 300 K: (a) when the electron beam is parallel to the ion-beam direction, and (b) after the sample has been tilted 27° in the microscope.

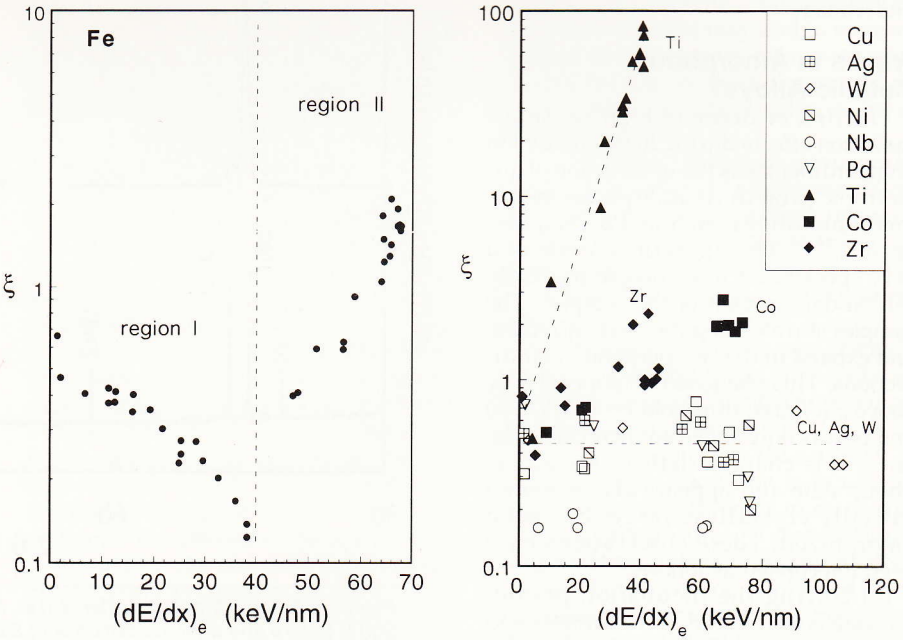

Figure 4. Damage efficiency $\xi = \sigma_d/\sigma_n$ as a function of the electronic slowing down $(dE/dx)_e$ for pure metallic ribbons irradiated at low temperatures with various GeV heavy (O to U) ions. See text for the meanings of regions I and II.

displacive $\alpha \leftrightarrow \omega$-transition,[23,24] the ω-phase is retained at room temperature and atmospheric pressure in a metastable state, which allows its observation. The aligned damaged zones visible after irradiation at low fluences might be premonitory signs of the phase transformation.

Other Metals

Zirconium is a metal that is very comparable to titanium. Note that these metals have similar phase diagrams.[23] Although strong damage is induced in Zr targets submitted to high $(dE/dx)_e$, as shown by electrical-resistivity measurements (Figure 4), no damage has ever been visualized in the electron microscope.[22] This indicates that only isolated defects or very small size-defect clusters are induced by electronic-energy deposition. These different behaviors can be explained by considering the fact that Zr is much heavier than Ti so that energy deposition must be much higher in Zr to induce lattice displacements. Some details concerning this point will be discussed later in the section But How Can Tracks Be Created in Metallic Targets?

Finally, signs of an irradiation-induced phase transformation similar to those observed in Ti have been detected in Be,[22] but because the high-pressure phase does not exist in a metastable state under normal temperature and pressure conditions, a low-temperature characterization of the new phase has to be undertaken.

Tracks in Amorphous Metallic Alloys?

The first evidence of high electronic excitation effects during high-energy ion bombardment was the observation of anisotropic growth in amorphous metal-metalloid alloys such as $Pd_{80}Si_{20}$ and $Fe_{85}B_{15}$.[25–27] This growth consists of a very spectacular macroscopic (typically ≈10%) deformation of the samples. The samples shrink along the beam direction and expand in the two perpendicular directions. This phenomenon appears only above a $(dE/dx)_e$ threshold (≈10 keV/nm) and occurs only above an incubation fluence. It is characteristic of the amorphous state and appears also when an initially crystalline target has been amorphized. These observations have been interpreted as follows:[28,29]

(1) During the incubation period, damage is introduced in the samples and additional free volume is created in the amorphous structure.

(2) The anisotropic growth results from a rocking motion of pairs of atoms that become oriented perpendicularly to the ion-beam direction. The driving force for such movements results from the shock wave that propagates radially around the ion trajectory (see next section).

It seems reasonable to suppose that, as these effects result from the high-energy deposition in electronic excitation that is localized in the close vicinity of the ion path, the damage introduced during the incubation period should lie inside cylindrical zones surrounding the ion trajectories. These "tracks," consisting of damaged amorphous matter surrounded by an amorphous matrix, are of course not visible in an electron microscope. Recently, however, it was shown that it is possible to perform chemical etching of low-fluence irradiated metallic glasses.[30] It is observed that etch cones can be formed at the places where "tracks"

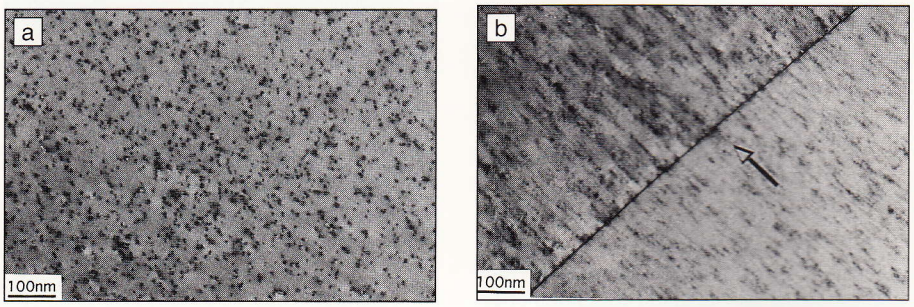

Figure 5. Bright-field electron micrograph of a titanium sample irradiated at 20 K with 2.2 GeV uranium ions up to a fluence of 2.5 × 10^{11} cm^{-2}. (a) The electron-beam direction is parallel to the ion beam. (b) The sample is tilted 20° in the electron microscope. The arrow indicates the projection of the ion-beam direction.

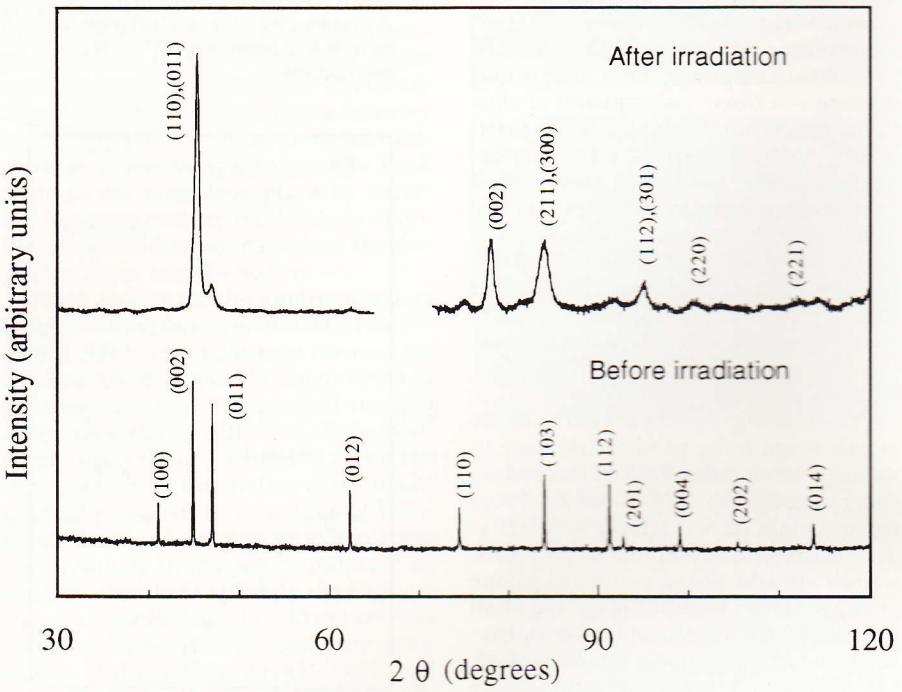

Figure 6. X-ray diffraction patterns (i.e., $\lambda(CoK_{\alpha_1})$) of a titanium sample registered at 300 K before and after irradiation with 2.2 GeV uranium ions up to a fluence of 1.2 × 10^{13} cm^{-2}. Before irradiation, all the observed diffraction lines belong to the hcp α-phase and are indexed in the lower part of the diagram. After irradiation, new peaks appear. They all correspond to the hexagonal ω-phase and are indexed in the upper part of the diagram.

come to the sample surface. It has not been possible to etch completely the inside part of the damaged cylinders due to an insufficient difference in the etching rates of damaged and undamaged matter. The observed surface pore density, when observed, corresponds to the impinging ion fluence. Finally, it should be emphasized that the threshold for track etching in such materials is much higher than the threshold for damage creation by electronic effects (respectively, 34 and 13 keV/nm in $Fe_{81}B_{13.5}Si_{3.5}C_2$).[30]

But How Can Tracks Be Created in Metallic Targets?

The creation of latent tracks in a metallic target is rather difficult to explain, as: (1) the numerous mobile-conduction electrons favor a rapid spreading of the deposited energy and an efficient screening of the space charge created in the vicinity of the projectile, and (2) we are obviously dealing with collective processes. To understand how extended defects can be created under high electronic excitations in metals, let us go back to the slowing down of energetic projectiles in matter. When an energetic ion penetrates a target (1) strong ionization of the target atoms located in the close neighborhood of its path occurs and (2) showers of excited electrons (δ-electrons or δ-rays) are ejected. A very high space-charge density is thus created in a localized region. What happens next is directly related to the nature of the target and depends mainly on the lifetime of the excited states, which governs the efficiency of the energy conversion into nuclear motion. In a metallic target, the lifetime of the space charge is limited by the rapid screening of the conduction electrons, contrary to what happens in insulators.

Two different models were often proposed to account for defect creation:

(1) The "thermal-spike" model, which was invoked years ago to account for damage creation in insulating materials.[31] More recently, an extension to metallic targets has been proposed.[32] In this model, the main concern is the conversion of the kinetic energy transmitted to δ-electrons into lattice vibrations via electron-phonon coupling. The resulting heating up of the lattice might very well account for the defect recombination and annealing described in the section on Tracks in Pure Metals. However, it would be difficult to explain with such an approach all the damage creation encountered in metallic targets.

(2) The "ion-explosion-spike" model, which was invoked years ago to account for damage creation in insulators[1] and organic materials.[33] In insulators, the electrostatic potential energy resulting from the ionization of the atoms is not screened. The recoil energy E_r due to Coulomb repulsion can reach high values (up to a few 10 eV), which are sufficient to induce individual lattice displacements. In metallic targets, the efficient screening of the positive charges by the numerous free conduction electrons makes such individual processes inoperant. However, a Coulomb explosion model has been recently applied to metallic targets when the space charge resulting from the ionization of the atoms is continuous along the ion path.[34] The cylinder of highly ionized matter surrounding the ion path is very unstable. The radial kinetic energy E_r conveyed to the charged ions through Coulomb repulsion depends mainly on the density and lifetime of the space charge. In metallic systems,[34] the lifetime of the space charge is limited by the response time t of the conduction electrons to an electrostatic perturbation. Time t related to the plasma frequency ω_p ($t \geq \omega_p^{-1} \approx 10^{-16}$ s) is much shorter than the characteristic phonon vibration time (10^{-13} s). The radial impulse received by all the atoms in the vicinity of the ion path corresponds to $E_r \approx 0.1$ to a few eV,[34] a much smaller amount than in insulators. But, due to the very short time (a few 10^{-18} s) spent by an ion to travel an interatomic distance, all the atoms lying in the vicinity of the ion trajectory are collectively repelled in a coherent way. The energy required to induce structural modifications in such a collective process is much lower than that needed in individual energy transfers. This point was checked and confirmed using molecular-dynamics simulations.[35,36]

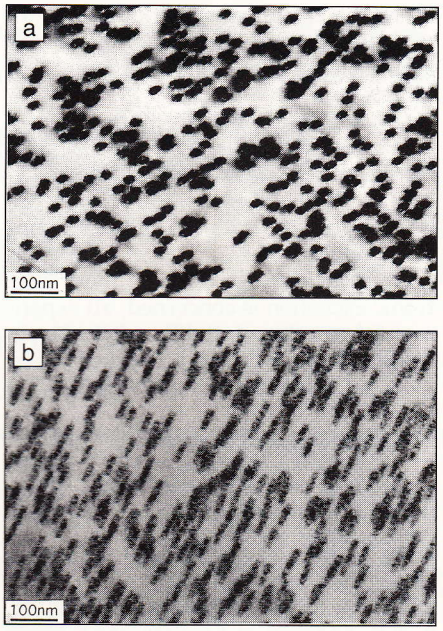

Figure 7. Bright-field electron micrographs of titanium irradiated at 300 K with 18 MeV C_{60} projectiles up to a fluence of 6×10^{10} cm^{-2}. (a) The electron-beam direction is parallel to the ion beam. (b) The sample is tilted 30° in the electron microscope.

In these Coulomb explosion models, it must be noted that the pertinent quantity is not the linear rate of energy loss $(dE/dx)_e$ but the linear rate dJ/dx of energy deposited in ionization processes.

This last mechanism seems particularly well-adapted to interpret all the results presented in this article. In particular, as the energy transfers are coherent in space and time, the response of the target can be analyzed in terms of phonon excitations. It has been shown that this results in:

(1) The generation of a radial shock wave[34,37] that might favor damage creation in those materials that present various allotropic phases in the pressure-temperature diagram. This is the case for all the metals in which damage creation under high electronic excitations was demonstrated (Fe, Ti, Zr, Be, etc.);
and/or

(2) A strong excitation of soft phonon modes when present.[38] The existence of soft phonon modes may lead to large amplitude displacements even with small energy excitations. Such dynamical disorder creates favorable conditions for defect formation.

Finally, the "ion-explosion-spike" mechanism detailed in Reference 34 predicts that damage creation in metals will be easier for: (1) low atomic-mass-number targets, (2) high atomic-number projectiles, and (3) low velocity projectiles.

Point (1) might explain why tracks are observed in a light target such as Ti, and not in Zr, although Ti and Zr are remarkably similar in other points.

Concerning points (2) and (3), the most favorable condition is to use uranium projectiles. In order to reach sufficient levels of energy deposition in electronic excitation using monoatomic beams, however, one is obliged to use high-velocity projectiles. In order to see the influence of point (3), the use of cluster beams can be very helpful. A first experiment has been performed very recently using 18 MeV C_{60} projectiles to

bombard Ti and Zr targets at 300 K.[39]

After cluster-ion irradiation of Ti targets (Figure 7), very large tracks are observed. The damage is quasicontinuous and is located inside ≈20 nm-diameter cylinders around the projectile path, which has to be compared with the discontinuous damage located within a cylinder of only ≈5 nm diameter after GeV Pb or U irradiation (Figure 5).

In the case of Zr targets, the results are even more spectacular. After fullerene irradiations, strongly damaged cylindrical zones are seen whereas after GeV U irradiation, no damage is visible in the electron microscope.

Although the rates of linear energy deposition in electronic excitation $(dE/dx)_e$ are close using both types of projectiles, the much larger extension of the damaged zones after cluster irradiations might result from the strong spatial localization of the deposited energy during the slowing-down process. The deposited *energy density* is related to the projectile velocity through the maximum range of the δ-electrons (some 1,000 nm using GeV Pb or U ions, a few interatomic distances using 18 MeV fullerene beams). The density of deposited energy during fullerene irradiations then reaches values as high as 100 eV/atom. The relaxation of such a high-energy density induces the spectacular modifications observed in this first experiment.

Conclusion

The experiments presented here show that high levels of energy deposition in electronic excitation are able to damage quite a few metallic targets and that such type of damage is no longer restricted to insulators. The difference between these two types of targets lies mainly in the thresholds above which these effects are encountered: a few keV/nm in insulators, ≈40 keV/ nm in most metallic targets.

Damage creation in metallic targets under electronic excitation involves collective effects and has been encountered in pure metals as well as in intermetallic compounds. Two indications come from the available results:

(1) The existence of various stable or metastable phases favors damage creation and track formation in metallic targets, and

(2) Tracks are formed more easily in low local symmetry compounds. This influence of the crystallographic structure, which is obvious, for example, in NiTi targets, has not been completely understood until now.

As far as damage creation under electronic excitation is concerned, all experimental results available until now in metallic targets can be accounted for by the Coulomb explosion spike model.

References

1. R.L. Fleischer, P.B. Price, and R.M. Walker, *J. Appl. Phys.* **36** (1965) p. 3645; *Nuclear Tracks in Solids* (University of California Press, Berkeley, 1975).
2. T.S. Noggle and J.O. Stiegler, *J. Appl. Phys.* **33** (1962) p. 1726.
3. K.L. Merkle, *Phys. Rev. Lett.* **9** (1962) p. 150.
4. H.H. Andersen, H. Knudsen, and P. Moller Petersen, *J. Appl. Phys.* **49** (1978) p. 5638.
5. H. Mori and H. Fujita, *Jpn. J. Appl. Phys.* **21** (1982) p. L494.
6. J. Koike, P.R. Okamoto, L.E. Rehn, and M. Meshii, *Metall. Trans.* **21A** (1990) p. 1799.
7. A. Barbu, G. Martin, M. Toulemonde, and J.C. Jousset, *C.R. Acad. Sci. Paris* **299** (1984) p. 409.
8. A. Barbu, A. Dunlop, D. Lesueur, and G. Jaskierowicz, in *Ordering and Disordering in Alloys*, edited by A.R. Yaravi (Elsevier, Amsterdam, 1992) p. 295.
9. A. Dunlop, D. Lesueur, J. Morillo, J. Dural, R. Spohr, and J. Vetter, *Nucl. Instrum. Methods* **B48** (1990) p. 419.
10. A. Barbu, A. Dunlop, D. Lesueur, and R.S. Averback, *Europhys. Lett.* **15** (1991) p. 37.
11. A. Dunlop, D. Lesueur, and A. Barbu, *J. Nucl. Mater.* **205** (1993) p. 426.
12. A. Audouard, E. Balanzat, S. Bouffard, J.C. Jousset, A. Chamberod, A. Dunlop, D. Lesueur, G. Fuchs, R. Spohr, J. Vetter, and L. Thomé, *Phys. Rev. Lett.* **65** (1990) p. 875.
13. A. Audouard, A. Dunlop, D. Lesueur, N. Lorenzelli, and L. Thomé (in press).
14. A. Barbu, A. Dunlop, J. Henry, D. Lesueur, and N. Lorenzelli, *Mater. Sci. Forum* **97–99** (1992) p. 577.
15. A. Barbu, A. Dunlop, G. Jaskierowicz, and N. Lorenzelli (in press).
16. A. Dunlop, D. Lesueur, and J. Dural, *Nucl. Instrum. Methods* **B42** (1989) p. 182.
17. A. Dunlop and D. Lesueur, *Radiat. Eff. Def. Sol.* **126** (1993) p. 123.
18. P. Legrand, A. Dunlop, D. Lesueur, N. Lorenzelli, J. Morillo, and S. Bouffard, *Mater. Sci. Forum* **97–99** (1992) p. 587.
19. A. Dunlop, D. Lesueur, P. Legrand, H. Dammak, and J. Dural, *Nucl. Instrum. Methods* **B90** (1994) p. 330.
20. J. Henry, A. Barbu, B. Leridon, D. Lesueur, and A. Dunlop, *Nucl. Instrum. Methods* **B67** (1992) p. 390.
21. H. Dammak, A. Barbu, A. Dunlop, D. Lesueur, and N. Lorenzelli, *Philos. Mag. Lett.* **67** (1993) p. 253.
22. H. Dammak, PhD dissertation, Ecole Polytechnique, 1994, published as CEA Report R 5668, H. Dammak, A. Dunlop, and D. Lesueur (NIMB) in press.
23. S.K. Sikka, Y.K. Vohra, and R. Chidambaram, *Prog. Mater. Sci.* **27** (1982) p. 245.
24. J.L. Murray, *Phase Diagrams of Binary Titanium Alloys* (ASM International, 1987).
25. S. Klaumünzer, G. Schumacher, S. Rentzsch, G. Vogl, L. Söldner, and H. Bieger, *Acta Metall.* **30** (1982) p. 1493.
26. S. Klaumünzer, Changlin Li, S. Löffler, M. Rammensee, G. Schumacher, and H.Ch. Neitzert, *Radiat. Eff. Def. Sol.* **108** (1989) p. 131.
27. A. Audouard, E. Balanzat, G. Fuchs, J.C. Jousset, D. Lesueur, and L. Thomé, *Europhys. Lett.* 3 (1987) p. 327; and *Nucl. Instrum. Methods* **B39** (1989) p. 18.
28. A. Audouard, E. Balanzat, J.C. Jousset, D. Lesueur, and L. Thomé, *J. Phys. Condens. Matter* **5** (1993) p. 995.
29. Ming-Dong Hou, S. Klaumünzer, and G. Schumacher, *Phys. Rev.* **B41** (1990) p. 1144.
30. C. Trautman, R. Spohr, and M. Toulemonde, *Nucl. Instrum. Methods* **B83** (1993) p. 513.
31. L.T. Chadderton and H. Montagu-Pollok, *Proc. R. Soc.* **A274** (1969) p. 239.
32. M. Toulemonde, C. Dufour, and E. Paumier, *Phys. Rev.* **B46** (1992) p. 14,362.
33. I.S. Bitensky and E.S. Parilis, *Nucl. Instrum. Methods* **B21** (1987) p. 26.
34. D. Lesueur and A. Dunlop, *Radiat. Eff. Def. Sol.* **126** (1993) p. 163.
35. P. Legrand, J. Morillo, and V. Pontikis, *Radiat. Eff. Def. Sol.* **126** (1993) p. 151.
36. P. Legrand, thesis (1993).
37. R. Bullough and J.J. Gilman, *J. Appl. Phys.* **37** (1966) p. 2283.
38. A. Dunlop, P. Legrand, D. Lesueur, N. Lorenzelli, J. Morillo, A. Barbu, and S. Bouffard, *Europhys. Lett.* **15** (1991) p. 765.
39. H. Dammak, A. Dunlop, D. Lesueur, A. Brunelle, S. Della-Negra, and Y. Le Beyec, *Phys. Rev. Lett.* **74** (1995) p. 1135. □